Replica Exchange Molecular Dynamics Modeling of Foldamers

Bamidele Adisa, David Bruce and Jay McAliley
Clemson University
127 Earle Hall
Clemson, SC 29634-0909
Phone: 864-656-5425
Fax: 864-656-0784

Introduction

Oligo(m-phenyleneethynylene)s, shown in Figure 1, have been shown to undergo a solvent-driven transition from a random conformation in low polarity solvents to an α-helix conformation in polar solvents as a result of solvophobic interactions.[1, 2] However, a detailed atomic-level study of the effects of specific intermolecular interactions, such as hydrogen bonding, van der Waals and Coulombic interactions between the aromatic side groups and various solvents have not been obtained.[3] Additionally, the elucidation of the significance of each of these phenomena experimentally is difficult; hence, molecular dynamics modeling techniques are the optimal way to study the formation and stability of helical secondary structures.

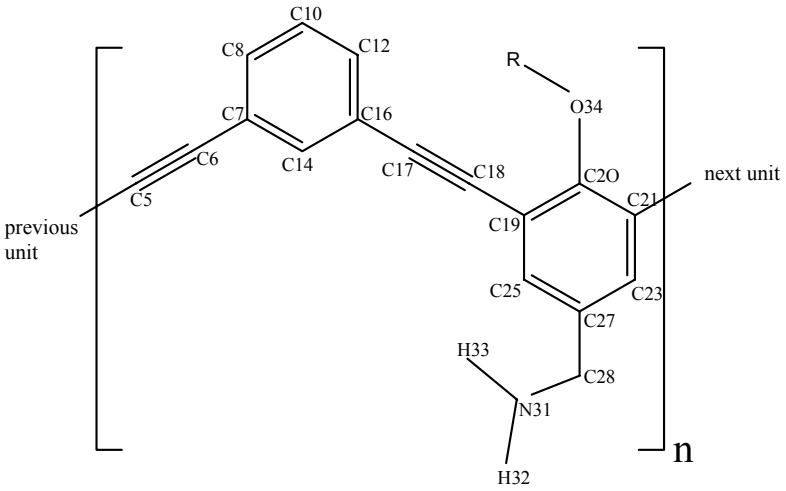

Figure 1. Monomeric unit of the oligomer. C5 is connected to C21 of the previous unit, while C21 is connected to C5 of the next unit. R is C_4H_9.

Molecular dynamics (MD) techniques are powerful tools for describing complex chemical systems at the atomic scale. These force field-based techniques provide an effective means for understanding and predicting macroscopic behavior that develops at time scales (1-100 ns) beyond those easily sampled by quantum computational methods. In an effort to better understand the inter-atomic forces influencing helices formation, this effort has focused on the results of MD and replica exchange MD simulations that examined the preferred conformations of phenyleneethynylene (PPE) oligomers having alkyl ether and amine functional groups attached to the oligomer backbone.

Methods

Replica Exchange MD

In this method, independent replicas of the original system are run simultaneously in parallel at different temperatures. At regular intervals, configurations are swapped following the Metropolis criterion[4]:

$$w_{ij} = \begin{cases} 1 & \text{for } \Delta \le 0 \\ \exp(-\Delta) & \text{for } \Delta > 0 \end{cases} \qquad (1)$$

where $\Delta \equiv \dfrac{(\beta_i - \beta_j)}{(E_j - E_i)}$

where *i* and *j* represent two adjacent replicas, w_{ij} is the transition probability for exchange between relicas *i* and *j*, $\beta = 1/kT$ and E is the potential energy. Figure 2 illustrates the replica exchange MD method.

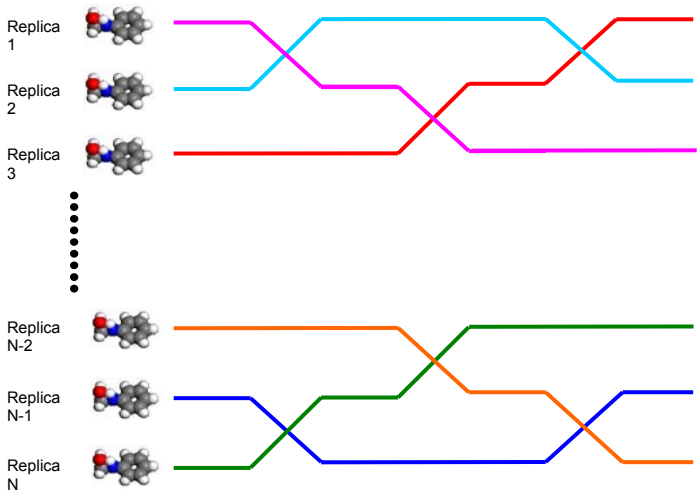

Figure 2: Replica exchange MD

The consequence of this replica exchange is that the high-temperature replicas help the low-temperature replicas to overcome energy barriers in the system. After each exchange, the velocities of atoms in each pair of replicas are rescaled by the square root of the ratio of the two temperatures.

Simulation Details

All MD studies used the Groningen Machine for Chemical Simulation (GROMACS, version 3.1.4) software package.[5, 6, 7] GROMACS employs a Message Passing Interface (MPI) parallelization method, which enables it to be used on cluster-type supercomputers (e.g., Beouwulf clusters). We examined the long-time dynamical behavior of the PPE oligomer in water using the GROMACS implementation of the OPLS all-atom[8] force field (OPLS-AA). Multiple MD simulations were performed using oligomers containing 12 residues in extended, random-coiled and helix conformations separately in water at 300 K, and the results from each of these simulations were compared. The results were analyzed to determine preferred conformation of the oligomer in aqueous solvent and what interactions were most important in the stabilization of the helix conformation.

In the simulations, the leapfrog algorithm was used to integrate Newton's equations of motion with a time step of 2 fs. Periodic boundary conditions were applied and non-bonded force calculations employed a grid system for neighbor searching. Neighbor list generation was performed after every 5 steps. A twin-range cut-off was used for the Lennard-Jones and Coulombic calculations. These calculations employed a cut-off radius of 0.9 nm for the short-range forces and a cut-off radius of 1.4 nm for the long-range forces. Initial velocities were randomly assigned from a Maxwell distribution at the selected simulation temperature. The temperature was controlled using Berendsen coupling[9], with a coupling constant of 0.1 ps. The LINCS algorithm[10] was used to constrain all bonds in non-water molecules. For water molecules, the SETTLE algorithm[11] was used to constrain bond lengths and angles to their equilibrium values. All MD simulations were continued for 5 ns and atomic trajectories were saved every 5000 steps for analysis.

Initial replica exchange MD simulations were run on 6 replicas of the oligomer, in extended conformation, in water, with T = 300-325 K. The temperatures of the replicas were selected such that the acceptance ratios between adjacent replicas were between 10% and 30%. Exchanges were attempted every 100 MD steps and atomic trajectories were stored before each exchange for further analyses. Each simulation was allowed to run for 500 ps.

Results and Discussion

Radius of Gyration

The radius of gyration gives a measure of the degree of compactness of a molecule. It can be calculated as follows:

$$R_g = \left(\frac{\sum_i \| r_i \|^2 \, m_i}{\sum_i m_i} \right)^{\frac{1}{2}} \qquad (2)$$

where m_i and r_i are respectively the mass of atom i and the position of atom i with respect to the center of mass of the molecule. Figure 3 shows the time evolution of the radius of gyration, Rg, for the helix, extended and coiled structures. It can be seen that the Rg for the helix structure remains steady throughout the MD simulation, with an average value of 0.83 ± 0.01 nm. This shows that it did not change significantly from its initial structure. However, the Rg for the extended structure shows a gradual decrease over the first 1 ns of trajectory and then reaches an average steady value of 0.94 ± 0.01 nm, while the Rg for the random-coiled structure shows a gradual decrease over the first 3.5 ns of trajectory before reaching an average steady value of 1.08 ± 0.02 nm. It is also important to note that the average Rg value for the helix is considerably lower than those for the extended and coiled conformations. This shows that the oligomer prefers the more compact helix conformation, shown in Figure 4, to the extended or coiled conformations when placed in an aqueous environment.

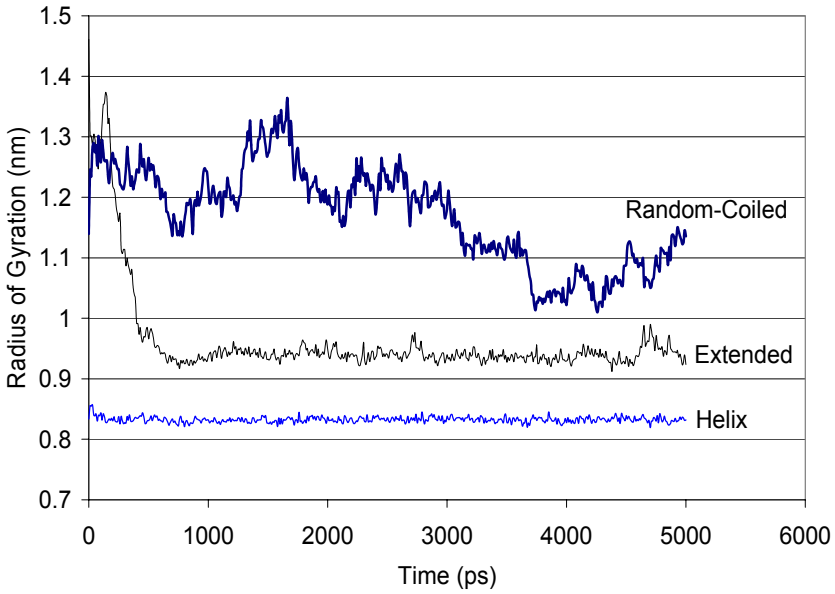

Figure 3. Time evolution of the radius of gyration (Rg) of the oligomer in the helix, extended and coiled conformations.

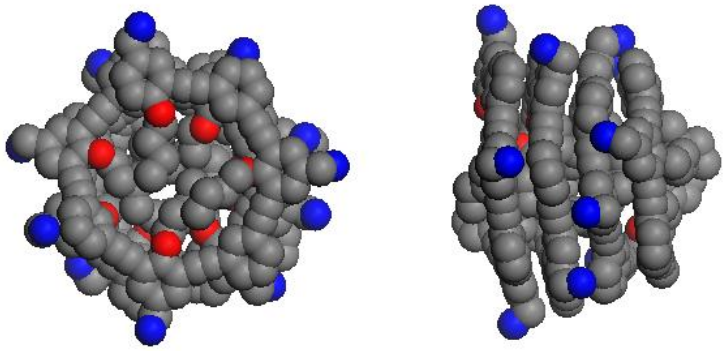

Figure 4. Top and side views for the PPE oligomer in energy-minimized helix conformation. Gray, red and blue colors represent carbon, oxygen and nitrogen atoms, respectively. Hydrogen atoms are not shown for clarity.

Potential Energy

Figure 5 shows the time evolution of the potential energies for the helix, extended and coiled structures. It shows the gradual lowering of the potential energies of the extended and coiled structures over the first 1 ns and 3.5 ns of trajectory respectively, after which average steady values of 1469.4 ± 48.6 kJ·mol^{-1} and 1613.6 ± 43.5 kJ·mol^{-1} are attained, respectively. This shows that the conformational irregularities present in the initial structures have been removed. Also, the potential energy of the helix structure is 1290.1 ± 44.2 kJ·mol^{-1}, which is lower than the potential energies of the extended and coiled structures. Therefore, we can deduce that the helix structure is the lowest energy conformation of the PPE oligomer in water, while the extended and coiled structures are each trapped in local energy minima.

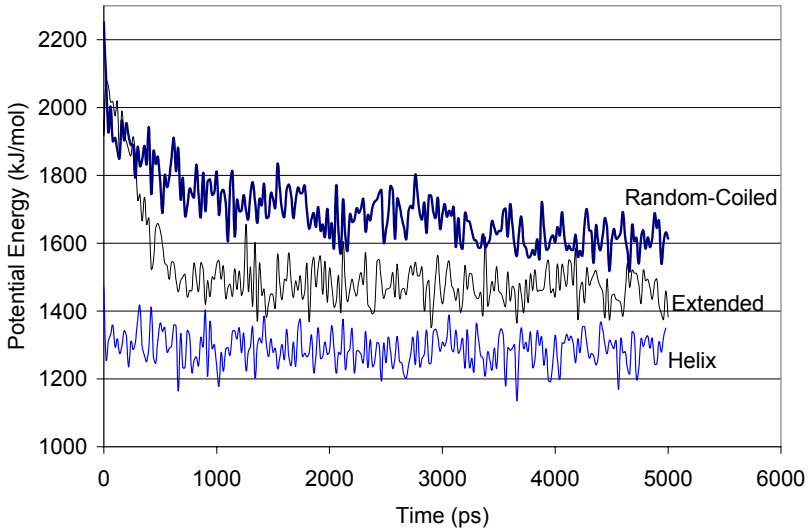

Figure 5: Time evolution of the potential energies of the oligomer in the helix, extended and coiled conformations.

Figure 6 shows the components of the potential energy of the oligomer in extended conformation. It can be seen that all the components of the potential energy, except the Lennard-Jones interactions, remain relatively constant over the course of the simulation. The Lennard-Jones interactions show a gradual decrease over the first 1 ns of trajectory until a constant value is attained, thus, this indicates that it is the main driving force for helix stabilization.

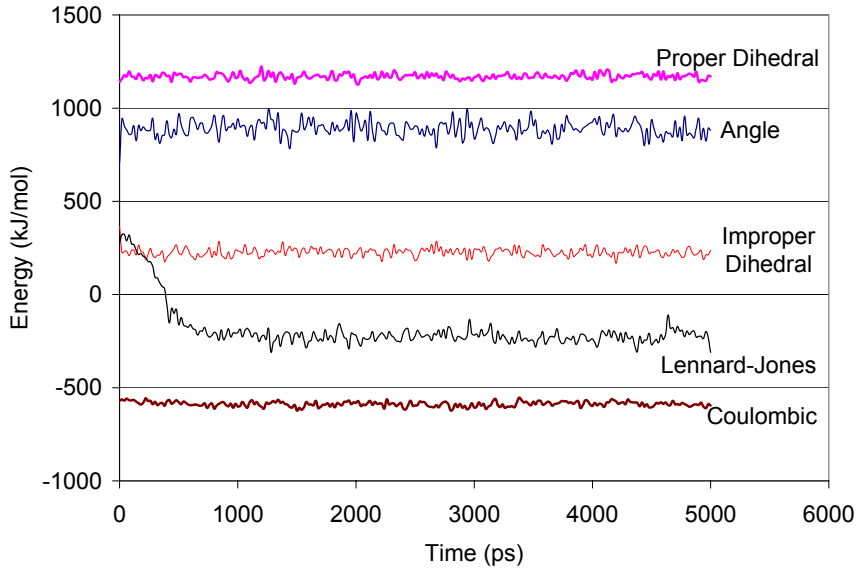

Figure 6: Time evolution of the components of the potential energy of the oligomer in the extended conformation.

REMD

Figure 7 shows the time evolution of evolution of temperature exchange for replica 3 (T=310 K) for the first 500 ps. It can be seen that there is random walk in *temperature space*

between the lowest and highest temperatures. Indeed, a similar behavior is observed for the potential energy, in which there is random walk in potential energy space between the lowest and highest energies (data not shown). Thus, we observe that replica exchange MD enables a wider sampling of conformation space.

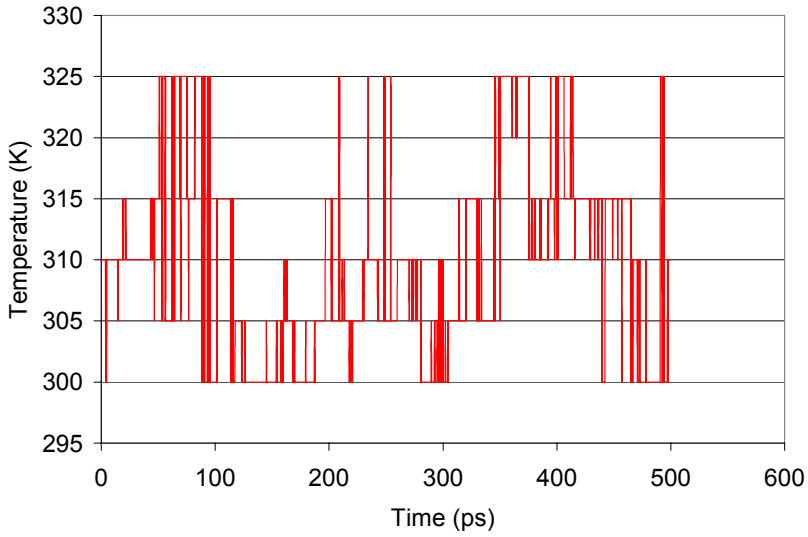

Figure 7: Time evolution of temperature exchange for replica 3 (T=310 K).

Conclusions

We have performed canonical and replica exchange MD simulations on phenyleneethynylene oligomers in water. The constant temperature simulations show that the oligomer prefers a helical conformation in water at room temperature, which is in agreement with previous experiments[1, 2]. Furthermore, we observed that the Lennard-Jones interactions are the main driving force for helices stabilization. A short replica exchange MD simulation was performed on the PPE oligomer in extended conformation to show that there is indeed exchange of configurations between replicas. Longer simulations are presently being run using the REMD method to investigate rate of helices formation.

References

1. Nelson, J. C.; Moore, J. S.; Wolynes, P. G.; Saven, J. G. *Science* **1997**, *277*, 1793–1796.
2. Prince, R. B.; Saven, J. G.; Wolynes, P. G.; Moore, J. S. *J. Am. Chem. Soc.* **1999**, *121*, 3114–3121.
3. Sen, S. *J. Phys. Chem. B*. **2002**, *106*, 11343–11350.
4. Sugita, Y.; Okamoto, Y. *Chem. Phys. Lett.* **1999**, *314*, 141-151.
5. Berendsen, H. J. C.; van der Spoel, D.; van Drunen, R. *Comp. Phys. Comm.* **1995**, *91*, 43–56.
6. Berendsen, H. J. C.; van der Spoel, D.; van Drunen, R.; van Buuren, A. R.; Apol, E.; Meulenhoff, P. J.; Tieleman, D. P.; Sijbers, A. L. T. M.; Feenstra, K. A.; Lindahl, E.; Hess, B., *Gromacs User Manual version 3.1.1*; Nijenborgh 4, 9747 AG Groningen: The Netherlands. Internet: www.gromacs.org (2002).
7. Lindahl, E.; Hess, B; van der Spoel, D. *J. Mol. Mod*. **2001**, *7*, 306–317.

8. Jorgensen, W. L.; Maxwell, D. S.; Tirado-Rives, J. *J. Am. Chem. Soc.* **1996**, *118*, 11225–11236.
9. Berendsen, H. J. C.; Postma, J. P. M.; DiNola, A.; Haak, J. R. *J. Chem. Phys.* **1984**, *81*, 3684–3690.
10. Hess, B.; Bekker, H.; Berendsen, H. J. C.; Fraaije, J. G. E. M. *J. Comp. Chem.* **1997**, *18*, 1463–1472.
11. Miyamoto, S; Kollman, P. A. *J. Comp. Chem.* **1992**, *13*, 952–962.